JOURNAL OF AIRCRAFT
Vol. 41, No. 2, March–April 2004

# Vortex Flow Visualization of a Yawed Delta Wing with Leading-Edge Extension

Myong Hwan Sohn* and Ki Young Lee†
*Korean Air Force Academy, Chungbook-Do 363-849, Republic of Korea*
and
Jo Won Chang‡
*Hankuk Aviation University, Kyonggi-Do 412-791, Republic of Korea*

**The development and interaction of vortices over a yawed delta wing with leading-edge extension (LEX) was investigated through off-surface flow visualization using micro water droplets and a laser beam sheet. Angles of attack of 12, 16, 20, and 24 deg were tested at sideslip angles of 0, −5, and −10 deg. The flow Reynolds number based on the main-wing chord was 1.82 × 10⁵. The wing vortex and the LEX vortex coiled around each other while maintaining comparable strength and identity at a zero sideslip. The increase of angle of attack intensified the coiling and shifted the cores of the wing and LEX vortices inboard and upward. By sideslip, the coiling, the merging and, the diffusion of the wing and LEX vortices increased on the windward side, whereas they became delayed significantly on the leeward side. Also the migration behavior of vortices on the windward and leeward sides of the wing changed considerably. The present study confirms that the sideslip angle has a profound effect on the vortex structure and interaction of a delta wing with LEX, which characterized the vortex-induced aerodynamic load.**

## Nomenclature

| | | |
|---|---|---|
| $c$ | = | wing root chord |
| $Re$ | = | Reynolds number, based on root chord |
| $s$ | = | local wing semispan |
| $x, y, z$ | = | coordinates of the wing-axes system, origin at the apex of the wing |
| $\alpha$ | = | geometric angle of attack |
| $\beta$ | = | sideslip angle |

## Introduction

THE delta wing with strake or leading-edge extension (LEX) is known to improve the aerodynamic performance of a delta wing at high angles of attack. The improvement results because the vortices generated by the strake or LEX interact with the vortices generated downstream by the main wing, reinforcing the lift generation and delaying the onset of the vortex breakdown. However, the situation is more complicated, and the results are not always in better aerodynamic performance, when the sideslip angle is not zero. At an angle of sideslip the effective sweep angles and the interaction state of the strake and wing vortices are different on the windward and leeward sides. The strake and wing vortices break down at much lower angles of attack on the windward side. The suction pressure distribution on the upper wing surface changes dramatically both in the chordwise and spanwise directions, which causes a pitching- and rolling-moment instability of the delta-wing configuration at sideslip. The complicated vortical flow at sideslip of a delta wing with strake requires more research in order to fully exploit the vortex lift.

There have been a number of studies of the vortex flow over a delta wing with strake or LEX. Erickson et al.[1] performed a series of pathfinder experiments with a 65-deg cropped delta wing, with and without LEX, at freestream Mach numbers from 0.40 to 1.60. Their extensive data and analysis greatly improved the understanding of the vortex development, interaction, and breakdown characteristics of a delta wing with LEX at a zero sideslip. Olsen and Nelson[2] investigated the vortex interaction of a delta wing with strake, and they reported that the interaction of the strake and wing vortices delayed the onset of vortex breakdown at the wing trailing edge to an angle of attack 10 deg greater than a single delta wing with the same sweep angle. They also observed that a lopsided coiling occurred with the stronger strake vortex and the weaker wing vortex at a zero sideslip. Grismer and Nelson[3] investigated the aerodynamic characteristics in yaw of a double-delta wing with strake-sweep and wing-sweep angles of 80/60 deg for angles of attack up to 40 deg. The effects of sideslip and the dynamic pitching rate were examined through the off-surface flow visualization and the force and moment balance measurements. They reported that the model exhibited static roll stability for lower angles of attack, but for higher angles of attack significant negative roll moments were generated at all sideslip angles tested (0, −3, and −6 deg). Hebbar et al.[4] investigated how the vortex breakdown characteristics at sideslip of a double-delta wing were affected by a modest planform-juncture modification through a water-tunnel flow visualization. They showed that at a constant angle of attack, as the sideslip angle increased, the windward strake vortex trajectory moved inboard with its breakdown point moving upstream, whereas the leeward strake vortex trajectory moved outboard with its breakdown point moving downstream. Verhaagen[5] investigated the effects of the Reynolds number on the vortex flow over a double-delta wing with strake-sweep and wing-sweep angles of 76/40 deg. He reported that the Reynolds number had little effect on the vortex flow over the strake portion, but the Reynolds number had a strong effect on the interaction between the strake and wing vortices over the wing portion, especially for the Reynolds number below $10^5$. Ericsson[6] presented a distinctive analysis on the rolling-moment characteristics of a pitching double-delta wing and the physics of the relevant vortex flow. Ericsson concluded that the lateral aerodynamics at high angles of attack was dominated by the interaction between the strake and wing vortices and the associated vortex breakdown.

The present study examines the vortical flow at sideslip of a delta wing with LEX through off-surface visualization of the wing

Presented as Paper 2002-3267 at the 20th Applied Aero Conference; received 31 July 2002; revision received 9 July 2003; accepted for publication 17 July 2003. 

*Professor, Department of Aerospace Engineering; myongsohn@hanmail.net. Senior Member AIAA.
†Associate Professor, Department of Mechanical Engineering.
‡Assistant Professor, Department of Aeronautical Science and Flight Operation. Member AIAA.

leeward flow region. The off-surface flow-visualization technique used micro water droplets and a laser beam sheet. Angles of attack of 12, 16, 20, and 24 deg were tested at sideslip angles of 0, −5, and −10 deg. The flow Reynolds number based on the main-wing root chord was $1.82 \times 10^5$. The analysis is focused on how the structure and interaction of vortices depend on the angles of attack and sideslip.

## Experimental Model and Methods

### Experimental Model

Figure 1a shows the geometric dimension and photographs of the delta-wing-LEX model used in the present study. The model was a 65-deg delta wing with a sharp leading edge, obtained by beveling 25 deg on the lower surface, while leaving the upper surface flat. The trailing edge was beveled in the same way. The model was a flat wing made of bakelite plate. The root chord was 530 mm including the LEX, the span 317 mm, and the thickness 15 mm. The LEX was also flat, made of a 6.35-mm-thick aluminum plate, and symmetrically beveled 25 deg at the leading and side edges. The model was supported by a balance strut located between 0.62c and 0.82c from the apex of the main wing. Figure 1b shows the experimental model in the test section of the wind tunnel. In the present study $x$ is the coordinate along the wing centerline measured from the wing apex, $y$ is the coordinate along the wing span measured from the wing centerline, and $z$ is the height above the upper wing surface.

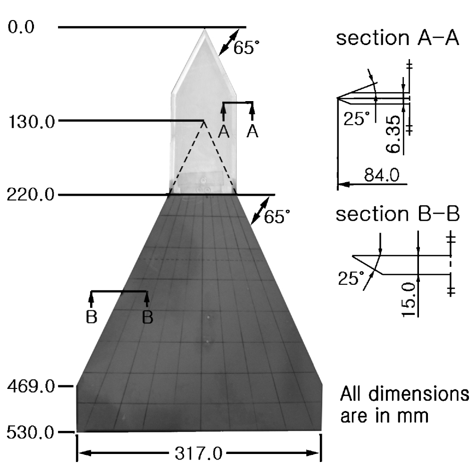


**a) Dimension of model**

**b) Model in test section**

**Fig. 1 Experimental model.**

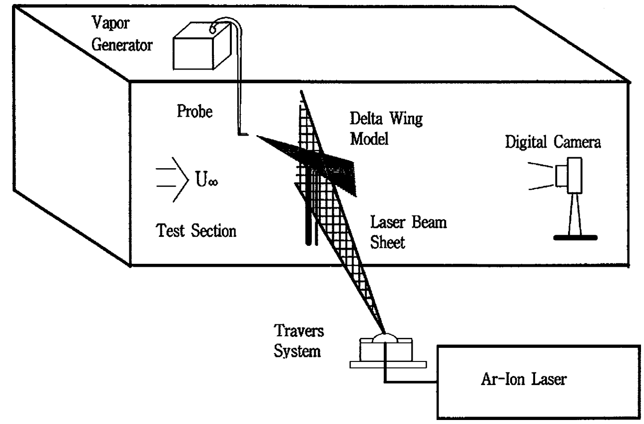


**Fig. 2 Off-surface flow-visualization experimental setup.**

### Off-Surface Flow Visualization

An off-surface flow-visualization method using micro water droplets and a laser beam sheet was developed in the present study. Figure 2 shows the experimental setup of the off-surface flow-visualization technique. Water droplets of 5–10 $\mu$m size were generated from a home-style ultrasonic humidifier. The water droplets exited just below the model apex and flowed with the airstream without any external power. The sedimentation distance of the visualization particle was calculated to be 0.256 mm at the trailing-edge station of the experimental model. A 3-W argon-ion laser was used to generate the light sheet. The laser light sheet made by 2 cylindrical lens and 2 convex-focusing lens was used to interrogate specific cross sections of the wing leeward flow region. The laser light sheet was perpendicular to the upper wing surface and the wing centerline. The illuminated planes were recorded by a high-resolution digital camera (SONY DCR-VX 2000 NTSC), at 30 frames per second. The camera was positioned 1.658 m behind the trailing edge of the experimental model, and the line of sight of the camera was parallel to the upper wing surface to avoid any distortion in the $z$ direction. The laser light sheet on the traverse platform was moved downstream at a constant speed while the camera was taking pictures at a shutter speed of 1/90 s. For each flow condition a total of 460 ∼ 480 frames were obtained while the laser light sheet was traveling from $x/c = 0.30$ to 1.0. The flow visualization was carried out in a low-speed wind tunnel at the Korean Air Force Academy, which had a test section 0.9 m high, 0.9 m wide, and 2.1 m long. The turbulent intensity was less than 0.3% for the available test-section speed range from 3.6 to 50 m/s. The flow Reynolds number was $1.82 \times 10^5$ based on the freestream velocity of 6.2 m/s and the main-wing root chord of 400 mm.

## Results and Discussions

Figure 3 shows section photos of the wing leeward flow region at $\alpha = 16$ and 24 deg at a zero sideslip. Two chord stations, $x/c = 0.30$ and 0.60, were taken. Figures 3a and 3b show that two distinct vortex pairs, each consisting of a larger LEX vortex and a smaller wing vortex, are developed in the leeward flow region of the wing at $x/c = 0.30$. The cores of the LEX and wing vortices at $\alpha = 24$ deg were more distinct than at $\alpha = 16$ deg. The mutual induction of the LEX and wing vortices having the same sense of rotation on each side of the wing moved the LEX vortex inboard and downward and the wing vortex inboard and upward initially. At $x/c = 0.60$ (Figs. 3c and 3d) the LEX vortex and the wing vortex of comparable strength spiraled around each other. The coiling of the LEX and wing vortices was more pronounced at the higher angle of attack, 24 deg. For example, as the LEX and wing vortices traveled downstream from $x/c = 0.30$ to 0.60, they completed about 170 deg rotation at $\alpha = 24$ deg, whereas they rotated only about 110 deg at $\alpha = 16$ deg. The coiling of the LEX and wing vortices continued, and they eventually merged into a single vortex at the wing trailing-edge station at $\alpha = 24$ deg (not shown in Fig. 3). The migration pattern of vortices while traveling downstream and the more pronounced coiling

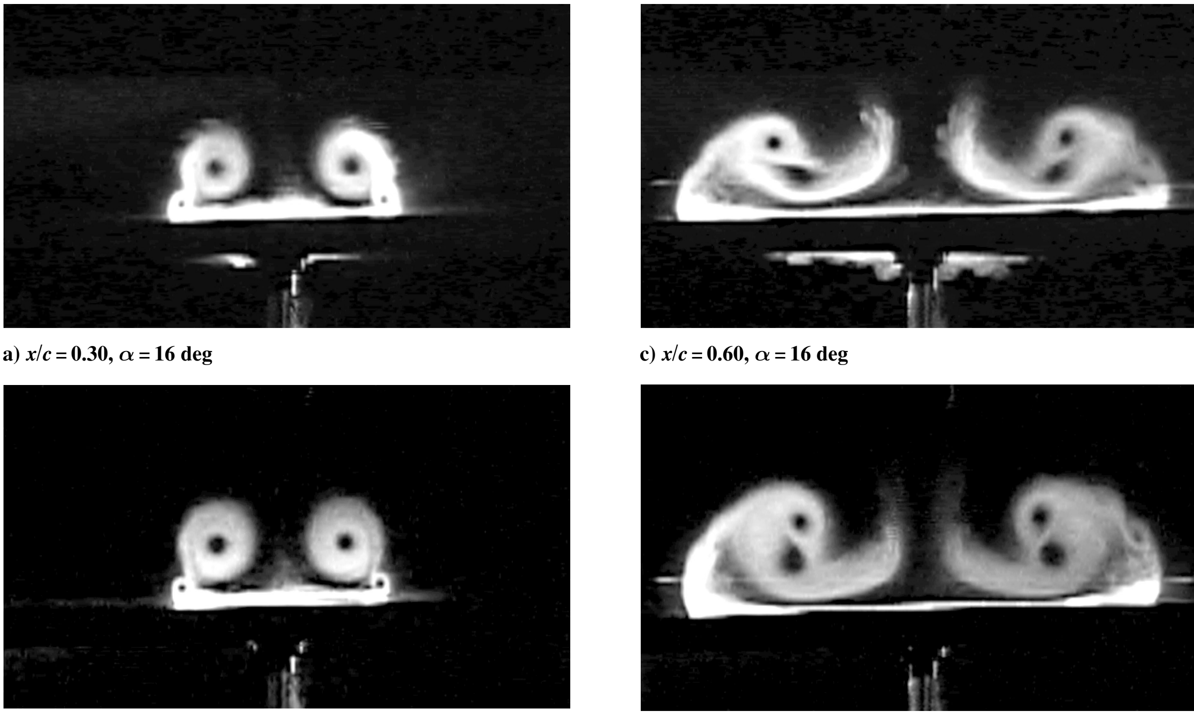

a) $x/c = 0.30$, $\alpha = 16$ deg

b) $x/c = 0.30$, $\alpha = 24$ deg

c) $x/c = 0.60$, $\alpha = 16$ deg

d) $x/c = 0.60$, $\alpha = 24$ deg

**Fig. 3 Visualized section photographs of wing leeward flow region at $\alpha = 16$ and 24 deg.**

at the higher angle of attack observed in Fig. 3 supported the study of Erickson et al.[1]

Figure 4 shows the chordwise development and the interaction of the wing and LEX vortices at $\alpha = 24$ deg at zero sideslip. At $x/c = 0.30$ (Fig. 4a) the wing leeward flow region was dominated by the fully developed LEX vortices, and the wing vortices just started to develop in the vicinity of the wing leading edge. The vortex flows on the two sides of the wing (port and starboard sides) in Fig. 4 have fairly good symmetry. When going downstream, the wing vortex increased in strength and size by the feeding of vorticity of the same sign through the shear layer, which connected the wing vortex and the wing leading edge, as suggested by Hoeijmakers et al.[7] However, the strength of the LEX vortex decreased when going downstream, which was also confirmed by the total pressure field measurement of Sohn and Lee.[8] The wing and LEX vortices on each side of the wing corotated and migrated in the spanwise and normal directions according to the rule of mutual induction of a vortex pair with the same sense of rotation. At $x/c = 0.456$ (Fig. 4e) the wing and LEX vortices were positioned laterally with nearly the same vertical distance from the wing surface. The clockwise coiling of the wing and LEX vortices on the port side of the wing and the counterclockwise coiling of the wing and LEX vortices on the starboard side of the wing continued when flowing downstream. At $x/c = 0.605$ (Fig. 4h) the core of the wing vortex was located directly above the core of the LEX vortex. Thus, the wing vortex and the LEX vortex each rotated 90 deg while traveling from $x/c = 0.456$ (Fig. 4e) to $x/c = 0.605$ (Fig. 4h). The size of the wing and LEX vortices was comparable after $x/c = 0.605$. The last frames of Fig. 4 show that the wing and LEX vortices merge to make a single vortex without breakdown at the trailing-edge position ($x/c = 1.0$). It was observed that the LEX and wing vortices in Fig. 4 spiraled around each other while maintaining comparable strength and identity before they merged into a single vortex, which differed from the lopsided coiling of the stronger strake vortex and the weaker wing vortex observed by Olsen and Nelson[2] in their experimental model of 80/60-deg sweep double-delta wing with strake.

Figure 5 shows the section photos of the wing leeward flow region at different sideslip angles ($\beta = 0$, $-5$, and $-10$ deg) and four selected chord stations ($x/c = 0.30$, 0.43, 0.60, and 1.0). The angle of attack was 20 deg. At $x/c = 0.30$ (Figs. 5a–5c) the core of the LEX vortex moved inboard and closer to the wing surface on the windward side, whereas it moved outboard and farther from the upper wing surface on the leeward side as the sideslip angle varied from 0 to $-10$ deg. The core of the leeward LEX vortex was located outboard and upward considerably at $\beta = -10$ deg. With this position the leeward LEX vortex had little effect on the upper-wing-surface suction pressure. At $x/c = 0.43$ (Figs. 5d–5f) the windward wing and LEX vortices were located laterally with nearly the same vertical distance from the wing surface, which caused a single rounded suction pressure peak on the windward side as shown in Fig. 4c of Ref. 9. The inboard and downward movement of the LEX vortex and the coiling of the wing and LEX vortices were slightly increased on the windward side, whereas they were greatly delayed on the leeward side. For example, the line connecting the cores of the leeward LEX and wing vortices was nearly parallel to the wing surface at $\beta = 0$ deg (Fig. 5d), but it made about 60 deg to the wing surface at $\beta = -10$ deg (Fig. 5f). That is, a sideslip angle of $-10$ deg delayed the counterclockwise coiling of the leeward wing and LEX vortices by 60 deg. At $x/c = 0.60$ the windward wing vortex was located directly above the LEX vortex at zero sideslip (Fig. 5g), which resumed the sharp suction pressure peak as shown in Fig. 4e of Ref. 9. At $\beta = -10$ (Fig. 5i) the windward wing and LEX vortices coalesced and diffused, whereas the leeward wing and LEX vortices had distinct cores and floated away from the wing surface. At $x/c = 1.0$ the windward wing and LEX vortex pair merged into a single vortex without breakdown at $\beta = 0$ deg (Fig. 5j), but burst at $\beta = -10$ deg (Fig. 5l). The breakdown occurred first in the LEX vortex (not shown in Fig. 5). Grismer and Nelson[3] reported that their double-delta wing model at $\beta = -6$ had a positive rolling-moment coefficient up to $\alpha = 20$ deg and a negative one after $\alpha = 24$ deg, which exhibited a static roll instability at high angles of attack. The inboard and downward migration of the windward vortices and the outboard and upward migration of the leeward vortices, and also the earlier diffusion and breakdown of the windward vortices observed in Fig. 5, suggested the premise that the delta wing with LEX model of the present study also had the possibility of static roll instability reported in Ref. 3.

Figure 6 shows the overlapped frames of the stereographic section photos of the wing leeward flow region for three different sideslip angles ($\beta = 0$, $-5$, and $-10$ deg). The angle of attack

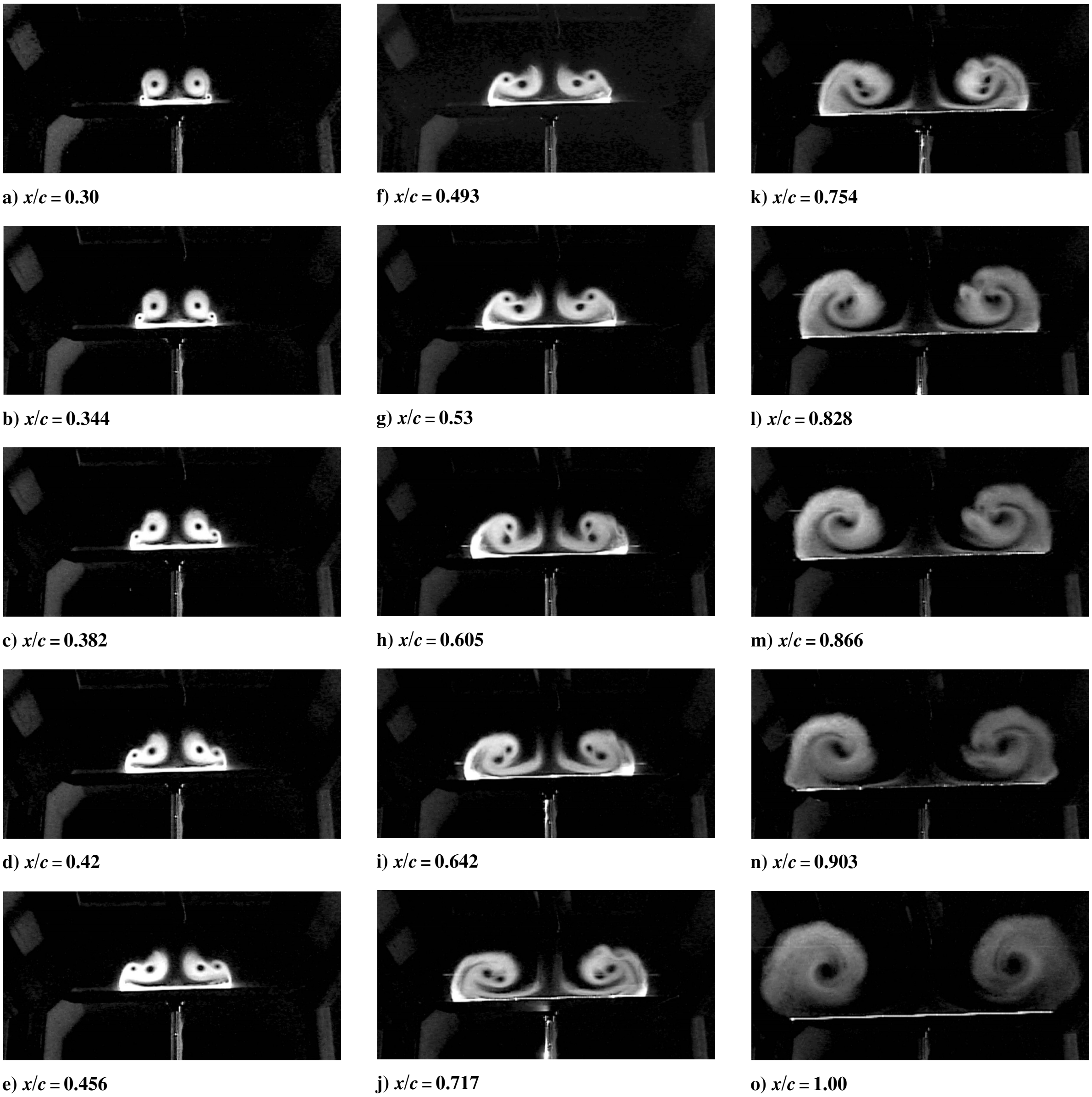


**Fig. 4 Chordwise development and interaction of the wing and LEX vortices ($\alpha = 24$ deg and $\beta = 0$ deg).**

was 20 deg. The stereographic photos were obtained from the dynamic images, which were taken by a camera positioned downstream of the wing trailing edge, with a "bird's eye view" (thus, the line of sight of the camera was not parallel to the wing surface), and a laser light sheet moving downstream at a constant speed. At zero sideslip (Fig. 6a) the upstream sections were dominated by the two pair of vortices, which were developed symmetrically on the port and starboard sides of the wing. Going downstream, the wing and LEX vortices spiraled each other and eventually merged into a single distinct vortex at the last section. At $\beta = -5$ deg (Fig. 6b) the wing and LEX vortices migrated more inboard, and their interaction and merging advanced on the windward side. The windward wing and LEX vortices completely merged into a single distinct vortex at the last section. The leeward wing and LEX vortices shifted outboard and upward, and their interaction and merging delayed greatly. At $\beta = -10$ deg (Fig. 6c) the windward wing and LEX vortices merged and diffused even at the midsections, whereas the cores of the leeward wing and LEX vortices were identified over almost the entire chord stations, which manifested the delayed merging and diffusion of vortices on the leeward side.

Figure 7 shows the trajectory of the core positions of the wing and LEX vortices of the two sides of the wing in the normalized $y$–$z$ plane, depending on angles of attack and sideslip. The starting position was in the 30% chord station. The chordwise interval was between $0.037c$ and $0.047c$. The center of the black dot in the visualization photos was assumed to be the vortex core position. Figure 7 shows that the windward wing vortex core started its trajectory in the vicinity of the port-wing leading edge and spiraled clockwise as it went downstream, while the leeward wing vortex core started its trajectory in the vicinity of the starboard-wing leading edge and spiraled counterclockwise as it went downstream. The LEX vortex core started its trajectory from the midspan position of the wing leeward flow region. The increase of angle of attack from 12 to 24 deg shifted the core positions of the wing and LEX vortices at zero sideslip inboard and upward as shown in Figs. 7a and 7b. At the larger angle of attack, the wing vortex core spiraled with a greater diameter, and the coiling of the wing and LEX vortices enhanced. At $\beta = -10$ deg (Figs. 7c and 7d) the increase of the angle of attack from 12 to 24 deg shifted the wing and LEX vortex cores almost vertically, especially on the leeward side. The amount of vertical shift was much greater than at zero sideslip angle. On the windward side with $\beta = -10$ deg (Fig. 7c), the cores of the wing and LEX vortices could not be traced beyond the midchord positions because of a breakdown with the larger 24-deg angle of attack.

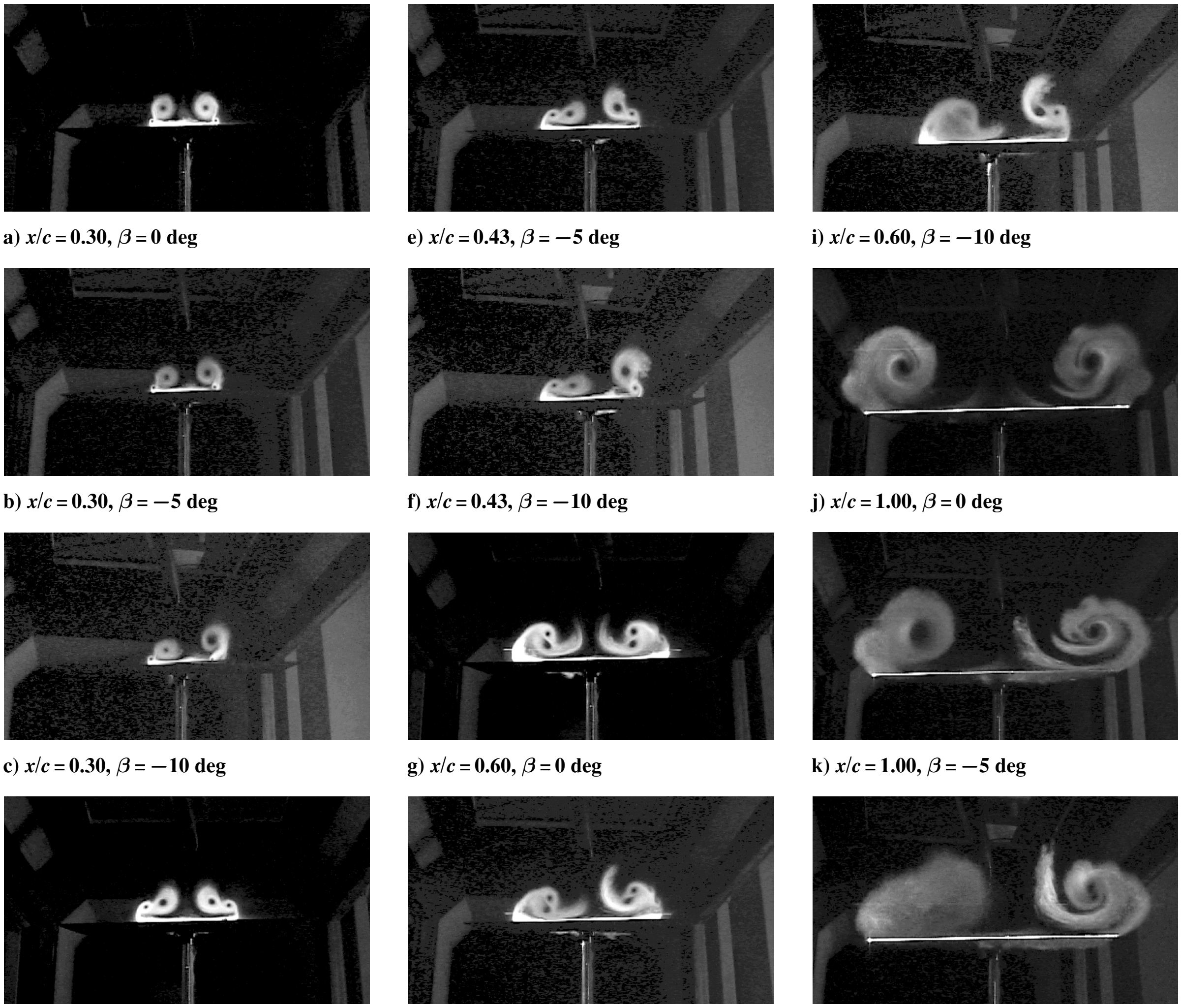

a) $x/c = 0.30$, $\beta = 0$ deg
b) $x/c = 0.30$, $\beta = -5$ deg
c) $x/c = 0.30$, $\beta = -10$ deg
d) $x/c = 0.43$, $\beta = 0$ deg
e) $x/c = 0.43$, $\beta = -5$ deg
f) $x/c = 0.43$, $\beta = -10$ deg
g) $x/c = 0.60$, $\beta = 0$ deg
h) $x/c = 0.60$, $\beta = -5$ deg
i) $x/c = 0.60$, $\beta = -10$ deg
j) $x/c = 1.00$, $\beta = 0$ deg
k) $x/c = 1.00$, $\beta = -5$ deg
l) $x/c = 1.00$, $\beta = -10$ deg

**Fig. 5 Effect of sideslip angle on the vortex development and interaction ($\alpha = 20$ deg).**

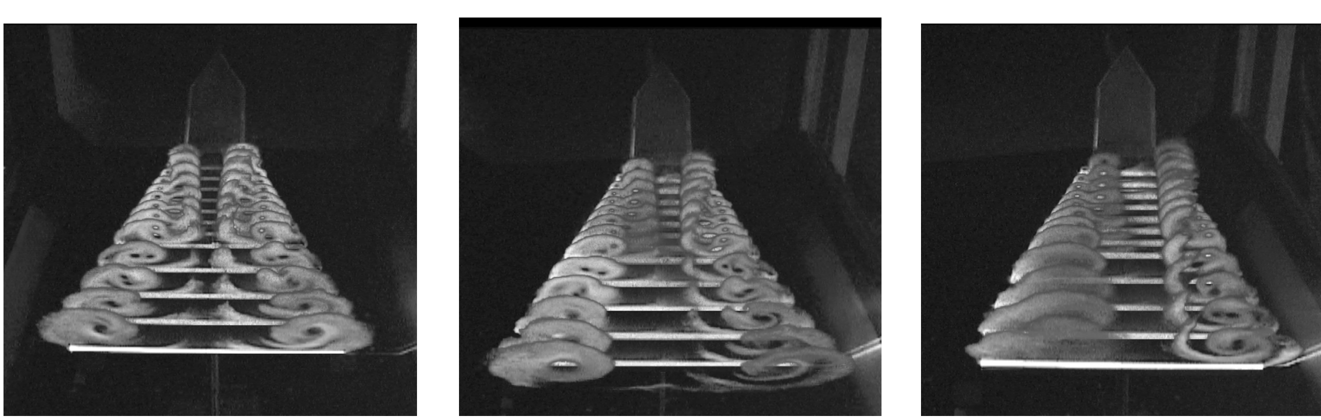

a) $\beta = 0$ deg
b) $\beta = -5$ deg
c) $\beta = -10$ deg

**Fig. 6 Stereographic section photographs of the wing leeward flow region ($\alpha = 20$ deg).**

Figure 8 isolates the effect of the sideslip angle on the vortex core trajectory at a fixed 20-deg angle of attack. The chordwise interval was between $0.02c$ and $0.04c$. On the windward side (Fig. 8a) the core of the port-wing vortex at zero sideslip started from $y/s \cong -0.91$ and $z/s \cong 0.15$ at $x/c = 0.30$, and the port-LEX vortex at zero sideslip entered the 30% chord section at $y/s \cong -0.58$ and $z/s \cong 0.51$. The port-wing vortex migrated inboard and upward, and the port-LEX vortex migrated inboard and downward initially, and then they coiled around each other as they went downstream. At the last chord station ($x/c = 1.0$) the position of the port-wing vortex core was $y/s = -0.70$ and $z/s = 0.32$. During travel from $x/c = 0.30$ to 1.0, the spanwise positions of the wing and LEX vortex cores crossed over twice at about $x/c = 0.60$ and 0.80 (not shown in Fig. 8). At $\beta = -10$ deg the core of the windward wing vortex started from $y/s \cong -0.79$ and $z/s \cong 0.18$ at $x/c = 0.30$, and the windward LEX vortex entered the 30% chord section at $y/s \cong -0.38$ and

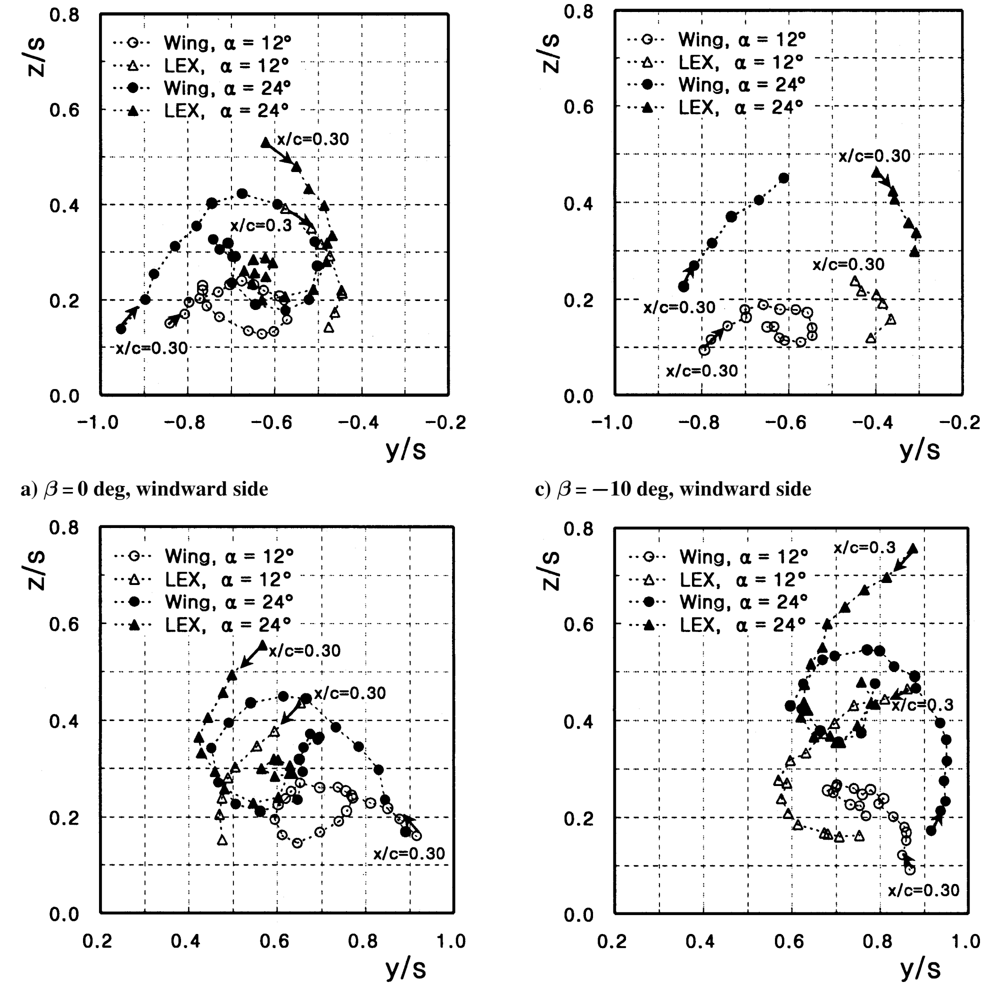


a) $\beta = 0$ deg, windward side

b) $\beta = 0$ deg, leeward side

c) $\beta = -10$ deg, windward side

d) $\beta = -10$ deg, leeward side

**Fig. 7 Vortex core trajectory in the *y–z* plane.**

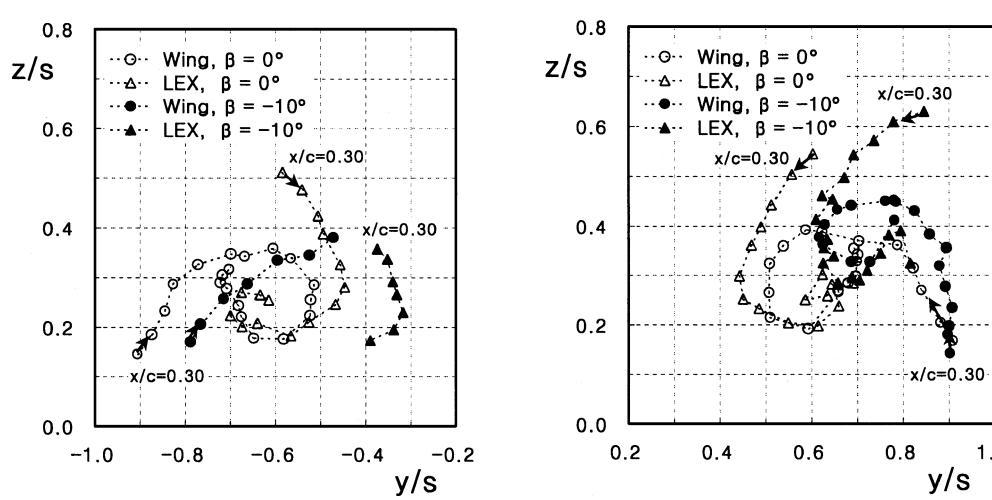


a) Windward side

b) Leeward side

**Fig. 8 Effect of sideslip angle on the vortex core trajectory ($\alpha = 20$ deg).**

$z/s \cong 0.38$. The windward wing and LEX vortices experienced a diffusion after the midchord, which made it impossible to trace the core positions. On the leeward side (Fig. 8b) the core of the wing vortex at zero sideslip started from $y/s \cong 0.90$ and $z/s \cong 0.17$ at $x/c = 0.30$, and the LEX vortex at zero sideslip entered the 30% chord section at $y/s \cong 0.60$ and $z/s \cong 0.54$. At $\beta = -10$ deg the core of the leeward-wing vortex started from $y/s \cong 0.90$ and $z/s \cong 0.14$ at $x/c = 0.30$, and the leeward-LEX vortex entered the 30% chord section at $y/s \cong 0.85$ and $z/s \cong 0.63$. Figure 8b shows that the sideslip angle of $-10$ deg shifted the wing and LEX vortices outboard considerably on the leeward side. The leeward-wing and LEX vortices coiled around each other without breakdown up to the last chord station. The spanwise positions of the cores of the leeward-wing and LEX vortices crossed over twice at about $x/c = 0.76$ and 1.0 as they were traveling from the 30% chord station to the wing trailing-edge station (not shown in Fig. 8).

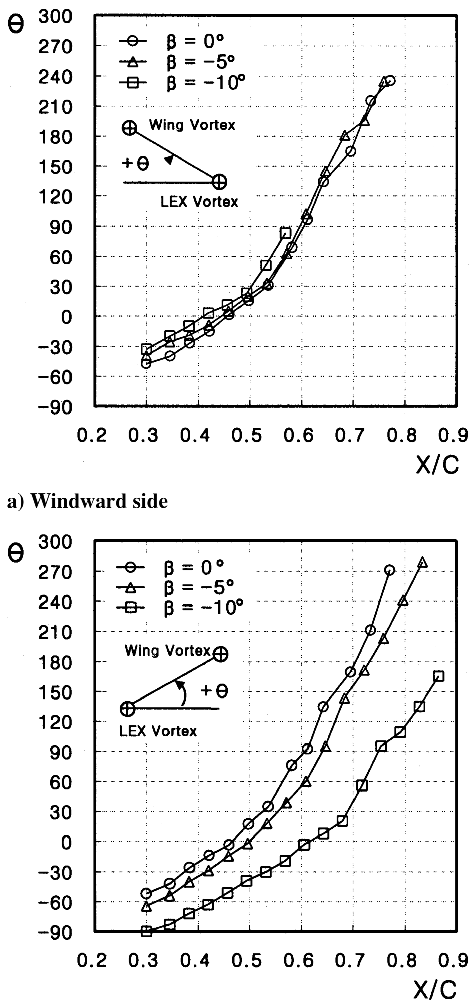


a) Windward side

b) Leeward side

**Fig. 9 Coiling angle variation with chordwise distance ($\alpha = 20$ deg).**

Figure 9 shows the coiling angle variation with chordwise distance at a constant 20-deg angle of attack. The coiling angle was defined as the angle between the reference line, which was parallel to the wing surface, and the line connecting the cores of the LEX and wing vortices. The positive coiling angle was measured clockwise from the reference line on the windward side and counterclockwise from the reference line on the leeward side, as shown by the legends in Fig. 9. Because of the unsteadiness of the vortex cores, the identification of vortex core positions had intrinsic errors. Also there was an observation error in measuring the coiling angle from the cut images of the dynamic visualization photos. Even though these errors had to be considered, the coiling-angle variation graph of Fig. 9 manifested the different interactions of the wing and LEX vortices on the two sides of the wing as a result of sideslip. On the windward side (Fig. 9a) the coiling angle of zero sideslip was about −48 deg at $x/c = 0.30$ and about 240 deg at $x/c \cong 0.77$. The coiling angle slightly increased at $\beta = -5$ and $-10$ deg. On the leeward side (Fig. 9b) the coiling angle of zero sideslip was about −52 deg at $x/c = 0.30$ and about 270 deg at $x/c \cong 0.77$. With $\beta = -10$ deg the coiling angle was about −90 deg at $x/c = 0.30$ and about 109 deg at $x/c \cong 0.79$. The coiling angle decreased considerably by sideslip on the leeward side. The coiling-angle variation characteristics of Fig. 9 demonstrated that by sideslip the interaction of the wing and LEX vortices increased a little on the windward side, whereas it became suppressed greatly on the leeward side. The greatly different coiling angle and vortex core trajectories on the windward and leeward sides of a yawed delta with LEX in the present study supports the conclusive arguments of Ericsson,[6] which stated that the sideslip has a profound effect on the vortex interaction and vortex-induced aerodynamic load of a delta wing with strake.

## Conclusions

A visualization study was conducted to analyze the development and interaction of vortices over a yawed delta wing with leading-edge extension (LEX). The wing vortex and the LEX vortex coiled around each other while maintaining comparable strength and identity at zero sideslip. The increase of angle of attack intensified the coiling and shifted the cores of the wing and LEX vortices inboard and upward. By sideslip, the coiling, the merging, and the diffusion of the wing and LEX vortices increased on the windward side, whereas they became delayed significantly on the leeward side. Also the migration behavior of vortices on the windward and leeward sides of the wing changed considerably. The present study confirms that the sideslip angle has a profound effect on the vortex structure and interaction of a delta wing with LEX, which characterized the vortex-induced aerodynamic load.

## Acknowledgment

This work was supported from the Basic Research Program of the Korea Science and Engineering Foundation (Grant Number R01-2000-000-00318-0).

## References

[1]Erickson, G. E., Schreiner, J. A., and Rogers, L. W., "On the Structure, Interaction, and Breakdown Characteristics of Slender Wing Vortices at Subsonic, Transonic, and Supersonic Speeds," AIAA Paper 1989-3345, Aug. 1989.

[2]Olsen, P. E., and Nelson, R. C., "Vortex Interaction over Double Delta Wings at High Angles of Attack," AIAA Paper 1989-2191, July 1989.

[3]Grismer, D. S., and Nelson, R. C., "Double-Delta-Wing Aerodynamics for Pitching Motions with and Without Sideslip," *Journal of Aircraft*, Vol. 32, No. 6, 1995, pp. 1303–1311.

[4]Hebbar, S. K., Platzer, M. F., and Chang, W., "Control of High-Incidence Vortical Flow on Double-Delta Wings Undergoing Sideslip," *Journal of Aircraft*, Vol. 34, No. 4, 1997, pp. 506–513.

[5]Verhaagen, N. G., "Effects of Reynolds Number on Flow over 76/40-Degree Double-Delta Wings," *Journal of Aircraft*, Vol. 39, No. 6, 2002, pp. 1045–1052.

[6]Ericsson, L. E., "Vortex Characteristics of Pitching Double-Delta Wings," *Journal of Aircraft*, Vol. 36, No. 2, 1999, pp. 349–356.

[7]Hoeijmakers, H. W. M., Vaatstra, W., and Verhaagen, N. G., "Vortex Flow over Delta and Double-Delta Wing," *Journal of Aircraft*, Vol. 20, No. 9, 1983, pp. 825–832.

[8]Sohn, M. H., and Lee, K. Y., "Experimental Investigation of Vortex Flow of a Yawed Delta Wing Having Leading Edge Extension," AIAA Paper 2002-3267, June 2002.

[9]Sohn, M. H., and Lee, K. Y., "Effects of Sideslip on the High-Incidence Vortical Flow of a Delta Wing with the Leading Edge Extension," AIAA Paper 2003-1107, Jan. 2003.